Surface & Coatings Technology 312 (2017) 32–36

Contents lists available at ScienceDirect

Surface & Coatings Technology

journal homepage: www.elsevier.com/locate/surfcoat

Surface modification of aluminium alloys by atmospheric pressure plasma treatments for enhancement of their adhesion properties

T.S.M. Mui [a,*], L.L.G. Silva [a,b], V. Prysiazhnyi [a], K.G. Kostov [a]

[a] Faculty of Engineering – FEG, Universidade Estadual Paulista – UNESP, Guaratinguetá, SP, Brazil
[b] Technological Faculty of Pindamonhangaba – FATEC, Pindamonhangaba, SP, Brazil

ARTICLE INFO

Article history:
Received 15 March 2016
Revised 6 July 2016
Accepted in revised form 8 August 2016
Available online 9 August 2016

Keywords:
Aluminium alloy
AA7075
Plasma
DBD
APPJ
Surface treatment

ABSTRACT

This work deals with surface modification of aluminium alloy AA7075 by two types of atmospheric pressure plasma: dielectric barrier discharge (DBD) and atmospheric pressure plasma jet (APPJ) with the purpose to enhance the adhesion of polyurethane coating on the alloy. The surface characterization was performed by using water contact angle, roughness and surface free energy measurements. Quality of the coating was tested according to the adhesion tape test (ASTM D3359) and evaluated by electrochemical techniques. The aluminium alloy showed great improvement of the surface wettability after plasma treatments. While, the adhesion tape test presented excellent results with perfect adhesion, meaning that both plasma treatments were efficient in improving the adhesion of the polyurethane coating to the AA7075. The Fourier Transform Infrared Spectroscopy (FTIR) results demonstrated that the plasma treatment cleaned the Al alloy surface by removing hydrocarbon contaminations. Both polarization curves and Electrochemical Impedance Spectroscopy (EIS) results showed better characteristics of corrosion resistance for polyurethane-coated AA7075 than untreated coated samples.

1. Introduction

Aluminium (Al) alloys have been one of the most employed materials in aircrafts structures, due to their light weight, high mechanical resistance, good corrosion properties and low cost. The 7000 series (Al—Zn—Mg—Cu) shows higher strength when compared to other classes of Al alloys. Therefore, they are specifically used in the fabrication of upper wing skins, stringers and stabilizers of aircrafts [1,2]. To endure critical conditions in aeronautic applications some chemical processes, such as, conversion coatings, anodizing and chromatization are often applied as pre-treatment for Al alloys to improve corrosion resistance and enhance adhesion properties. However, the hexavalent chromium [Cr^{+6}] generated by these techniques is known to be toxic and hazardous to humans and the environment. In order to find methods environmental-friendly with the same efficiency as the chromates, several researches have been developed to modify Al alloys for aeronautic and aerospace purposes [3–6].

Atmospheric pressure plasmas are clean and environmental-friendly type of process that can be easily applied in in-line production, the capital cost is relatively low when compared to other methods [7–9].

Dielectric barrier discharge (DBD) is considered one of the most popular cold atmospheric plasma sources that generates non-equilibrium plasma [10]. Typical DBD configuration consists of an electrode arrangement where one or both electrodes are covered by a dielectric material like glass, quartz or ceramics [11]. When a high voltage (typically tens of kV in the frequency range of 50–10^4 Hz) is applied between the electrodes, the gas breakdown occurs and a large number of short-lived current filaments, known as microdischarges appear in the inter-electrode gap. Most industrial applications of DBD operate in this filamentary mode [12]. DBD has been applied for ozone generation, sterilization, flat plasma displays, excimer UV lamps, surface modification [13], and most recently in biomedical [14] and agriculture [15] applications.

Atmospheric pressure plasma jet has recently been a topic of great interest, since it can generate non-equilibrium plasma in open space rather than in a confined discharge gap. The plasma jet operation usually depends on the working gas and on the electrical excitation, which can vary from DC power supply to sine-wave signal with frequency from tens of Hz to MHz (radio frequency) and to GHz (microwave) [16]. The separation of the generation region from the application region enables the direct exposure of thermosensitive substrates, including local treatment in complex geometries substrates [17]. Therefore,

* Corresponding author at: Department of Physics and Chemistry, Universidade Estadual Paulista Júlio de Mesquita Filho (UNESP), Faculdade de Engenharia de Guaratinguetá, Av. Ariberto Perreira da Cunha 333, Pedregulho, 12516410 Guaratinguetá, SP, Brazil.
E-mail addresses: taiana_mui@yahoo.com.br (T.S.M. Mui), leide.kostov@fatec.sp.gov.br (L.L.G. Silva), mr.vodik@gmail.com (V. Prysiazhnyi), kostov@feg.unesp.br (K.G. Kostov).

http://dx.doi.org/10.1016/j.surfcoat.2016.08.024
0257-8972/

plasma jets have been employed to materials surface modification [18] and in biomedical application (bacteria inactivation, cancer treatments and skin therapy) [19].

In this work, two types of atmospheric pressure plasmas (DBD and plasma jet) were used to pre-treat the aluminium alloy (AA7075) to enhance the adhesion of a polyurethane coating on the AA7075 alloy, avoiding the use of any chemical process typically applied in the industry. In this way the process becomes environmental-friendly, human contamination risks are reduced and the costs are decreased as well.

2. Materials and methods

Plasma treatments were performed on as-received aluminium alloy AA7075-T7351 (89.6% Al) with dimensions of Ø15 × 3 mm. No metallographic surface preparation was used to enhance the mechanic anchorage between the Al alloy surface and paint coating. Prior to plasma treatments, samples were ultrasonically cleaned in distilled water for 15 min and than in isopropyl alcohol for 10 min to remove contaminants from the surface. To evaluate the reproducibility of the experiments, all tests were done in duplicate.

The DBD reactor was consisted of two parallel aluminium electrodes with diameter of 9.5 cm, where both electrodes were covered by a Mylar sheet of 0.5 mm thickness. The bottom electrode was connected to a high-voltage source while the upper electrode was grounded. Plasma was generated by an AC power supply (60 Hz) in airflow (8 L/min). The inter-electrode gap was fixed to 4 mm and the applied voltage used was 30 kVp-p. Samples were exposed to air-DBD plasma for 5 min, 7.5 min, 10 min and 15 min. The schematic diagram of the DBD system can be found elsewhere [20].

Argon plasma jet was generated in a glass tube using a 16 mm horn-like nozzle. The nozzle to sample distance was fixed to 1 mm and the applied voltage used was 12 kVp-p. Samples were exposed to plasma for 20 s, 30 s, 40 s and 60 s. The plasma jet system details and experimental configurations are available in [21].

The AA7075 alloy surface characterization was carried out by measuring contact angle and surface free energy (SFE) with a Rame-Hart 300 goniometer, using the sessile drop method and the DropImage software, provided by the manufacturer. Deionized water and diiodomethane were used as test liquids, the volume of each liquid drop was set as 2 μL, the average value of at least 3 drops from each liquid was calculated (for each drop the contact angle was measured 5 times). SFE evaluation was performed using the Surface Free Energy tool in DropImage software, which is based on the Owens-Wendt model for two liquids (deionized water and diiodomethane) using the geometric mean method.

The chemical composition of the substrates was analyzed by Attenuated Total Reflectance Fourier Transform Infrared Spectroscopy (ATR-FTIR) performed on a PerkinElmer Spectrum 100 spectrometer. The spectra were acquired from 650 cm^{-1} to 4000 cm^{-1} with spectral resolution of 2 cm^{-1}. Each spectrum was obtained as an average of 40 scans.

After plasma treatments, samples were painted with polyurethane paint JETGLO® from Sherwin-Williams manufacturer. The painting was performed no more than 10 min after the treatments and dried in room temperature for 48 h prior to any measurement.

Quality of the coating was evaluated according to the adhesion tape test ASTM D3359 [22] and electrochemical techniques, which were performed by an AUTOLAB Potentiostat (302N) using a three electrode electrochemical cell, consisted of reference electrode (Ag/AgCl), counter-electrode (Pt) and working electrode (AA7075 alloy with area of 0.64 cm^2). All electrochemical experiments were conducted in 3.5% NaCl solution at room temperature, in the following order: Open Circuit Potential (OCP), Electrochemical Impedance Spectroscopy (EIS) and Polarization Curves (PC). Before any measurement all electrodes remained inside the electrochemical cell in immersion for 20 h to reach stationary conditions. After immersion time, the OCP was measured as a function of time for more 3 h. EIS spectra were collected from 10^5 to 10^{-2} Hz frequency range, using a perturbation signal of 10 mV and acquisition data scanning of 10 points per decade. Polarization curves were obtained with a potential scan rate of 0.33 mV/s from −1.2 V up to 0.6 V.

3. Results and discussion

3.1. Surface characterization (contact angle, SFE and FTIR)

Water contact angle values of the AA7075 alloy were affected significantly by both plasma treatments as can be seen in Fig. 1. Water contact angle of the control (CT) untreated sample was 89° ± 2°, whereas after plasma treatments water contact angle decreased up to 5° ± 1° and 19° ± 1° for DBD and plasma jet, respectively. Decrease of the contact angle values after plasma treatments was observed for both test liquids, water and diiodomethane.

On the other hand, AA7075 samples treated by DBD and plasma jet exhibited a substantial increase on the surface free energy (SFE) when compared to the CT sample. Fig. 2 shows SFE values of AA7075 samples for all conditions, before and after plasma treatments. SFE of plasma treated samples has similar value around 70 mJ/m^2, which is about 2.5 times higher than the one of control sample.

Although, the polar component exhibited the highest accession after plasma exposure, (around 10 times more than the CT sample), the dispersive component also tends to increase after plasma treatments. After plasma treatment, the Al alloy surface became more hydrophilic, as can be seen in Fig. 1 by the decrease of the water contact angle, resulting in a lager spread of the liquid drop on to the alloy surface. Similar results were found by some authors [23,24] using different arrangements of plasma sources and Al alloys. These authors inferred that the increase of the SFE polar component is due to the generation of polar groups on the Al alloy surface after plasma treatments.

The FTIR spectra for CT and plasma jet treated sample (60 s) are displayed in Fig. 3. Since the spectrum obtained for DBD treated samples was similar to the one of plasma jet, only one curve was inserted in the graph. Note that the signal intensity obtained from the aluminium alloy samples is very weak and in some wavenumber regions it is comparable with the noise generated by the ATR element (diamond crystal). Therefore, the region from 2390 to 1920 cm^{-1} was excluded from graph.

Control samples had several peaks that were related to surface hydrocarbon contaminants: CH_2/CH_3 vibration peaks (as. str. CH_3 at 2964 cm^{-1}, as. str. CH_2 at 2929 cm^{-1}, s. str. CH_3 at 2857 cm^{-1}, ass. bend. CH_3 at 1460 cm^{-1} and s. bend. CH_3 at 1376 cm^{-1}), C═O (str. 1742 cm^{-1}), and C═C (s. str 1649 cm^{-1}). The peak of H-bonded OH (3328 cm^{-1}) is related to the humidity condensation, while the

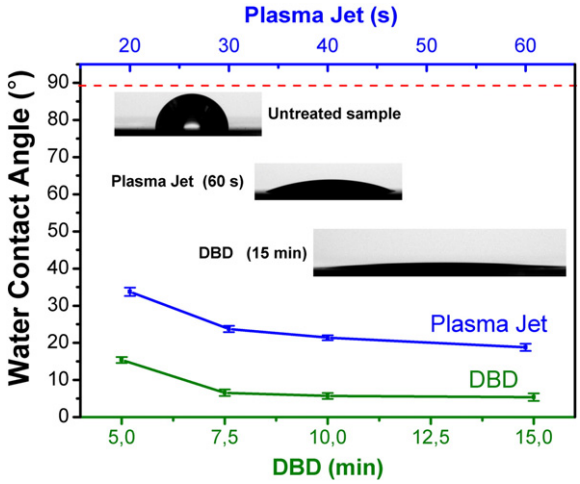

Fig. 1. Water contact angle values.

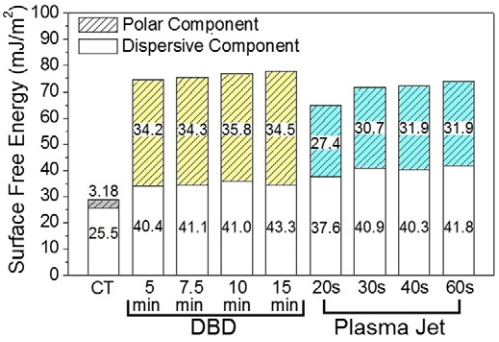

Fig. 2. Surface free energy before and after plasma treatments.

substrate is represented by the peak of Al—O/Al—OH (str. 948 cm^{-1}) [25–27].

After plasma treatments those characteristic hydrocarbon peaks and surface humidity were no longer detected, leaving only Al—O/Al—OH vibration peaks that represent the metal substrate. Typically, the removal of surface hydrocarbons and weak boundaries layers is associated to the enhancement of the SFE. The obtained results are in good agreement with the enhanced surface wettability.

3.2. Quality of the polyurethane coating

Quality of polyurethane (PU) coating with 85 μm ± 15 μm thickness on the AA7075 alloy surface was evaluated by ASTM D3359 method B and electrochemical techniques.

3.2.1. Adhesion tape test

Some results of the adhesion tape test can be seen in Fig. 4. On the control sample the PU paint came off completely from the squared area (see Fig. 4a), whereas for both plasma process for DBD treatment time above 5 min and plasma jet above 30 s led to perfect adhesion of the PU painting. In Fig. 4b is shown a photo of the DBD treated sample for 15 min.

Since the paint came off completely, the classification according to ASTM D3359 standard for CT sample was 0B. The samples treated with DBD (7.5, 10 and 15 min) and plasma jet (40 and 60 s) were classified as 5B with none paint detachments. The DBD (5 min) and plasma jet (20 and 30 s) treated samples were classified as 2B with paint removal around 15%. The adhesion tape test results are in accordance to the water contact angle, SFE, FTIR and roughness results. It means that the adhesion improvement occurred due to the Al alloy surface activation and cleaning and not because of surface roughening.

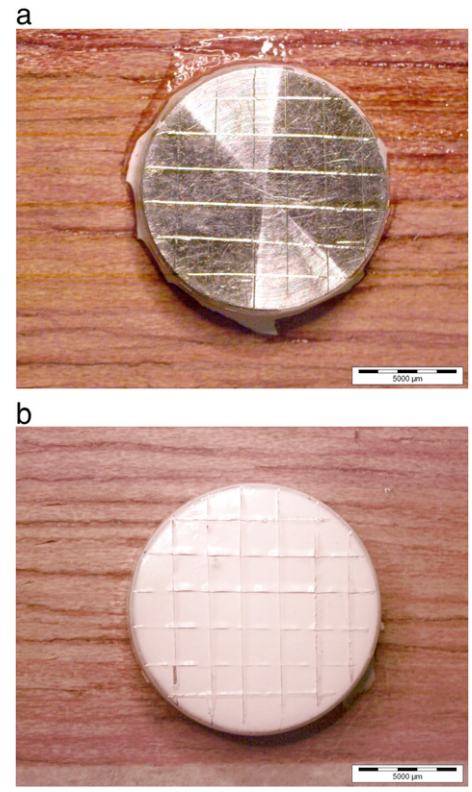

Fig. 4. Adhesion tape test result (a) CT sample (b) DBD treated sample for 15 min.

3.2.2. Electrochemical techniques

The corrosion behavior of the samples was analyzed by Open Circuit Potential (OCP), Electrochemical Impedance Spectroscopy (EIS) and Polarization Curves. Results of OCP as a function of the time are illustrated in Fig. 5. Similar behavior of constant potential with the time is observed for all samples.

However, OCP values of treated samples are more positive (noble) when compared to the CT sample, except for the plasma jet treated sample at 20 s, which potential is slightly more negative. All DBD treated samples (5 min, 7.5 min, 10 min and 15 min) got similar OCP values (−0.04 V) that are more positive than OCP values of plasma jet treated samples (−0.27 up to −0.18 V) and the CT sample (−0.26 V). In general, when the potential is higher means that the material is nobler and more resistant to corrosion. Though, as all samples were painted this difference in OCP values can be attributed to non-uniformity and adhesion of the painting layer on the substrate.

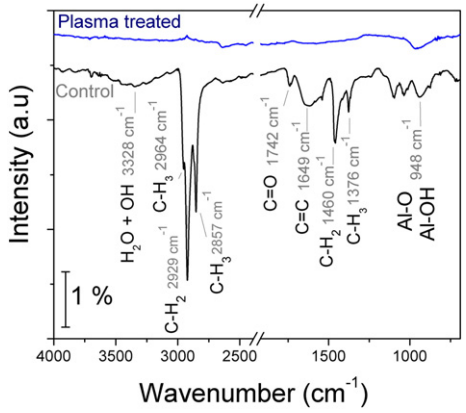

Fig. 3. FTIR spectra for plasma treated and CT conditions.

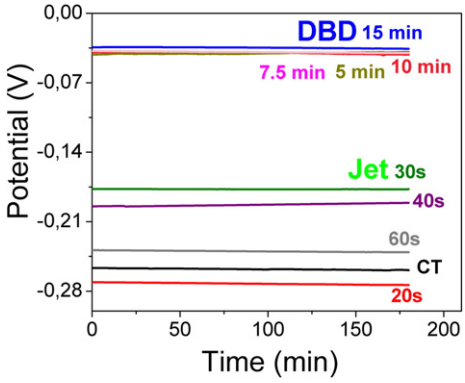

Fig. 5. OCP curves for all conditions.

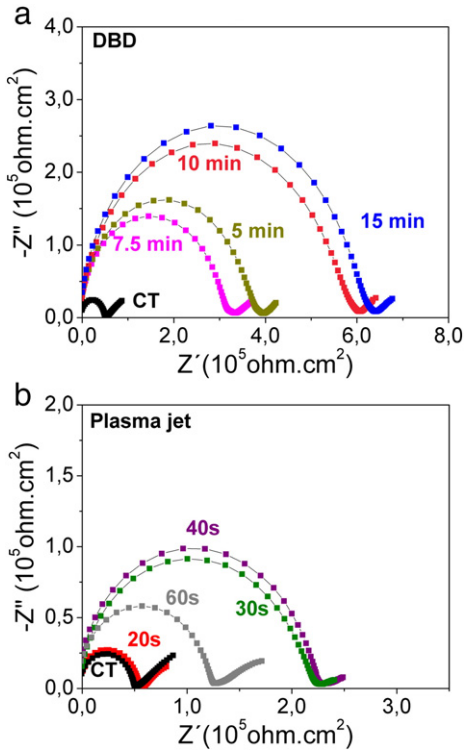

Fig. 6. Nyquist diagrams (a) DBD (b) plasma jet process.

After OCP measurements, the Electrochemical Impedance Spectroscopy analysis was conducted and the capacitance of the polyurethane layer on the Al alloy substrate was calculated. The Nyquist diagrams for CT, DBD and plasma jet treated samples are presented in Fig. 6.

Within the investigated frequency range, the Nyquist diagrams in Fig. 6a and Fig. 6b exhibited a similar behavior, a semi-circle and a diffusional element. The DBD treated samples presented the highest values of real and imaginary impedance (Z′ and Z″). The Z″ value obtained for DBD treated sample at 15 min was approximately 2.5 times higher than the one of the plasma jet treated sample for 40 s and around 10 times higher than the CT sample. However, the samples treated by plasma jet also showed impedance values, from 2 up to 5 times higher than the one of CT sample. This indicates that, the coating resistance on treated samples is higher than the untreated sample (CT) when exposed to 3.5% NaCl solution.

The coating capacitance (Cc) was calculated using the formula reported by some authors [28] and determined at 10 kHz frequency, because of the finding that at higher frequencies coating capacitance values tend to be more stable and reliable for calculation [29].

The calculated values of coating capacitance can be observed in Table 1. CT and plasma jet (20 s) samples have similar Cc values, around 7×10^{-10} F/cm^2. For other plasma jet (30, 40 and 60 s) and DBD (5, 7.5, 10 and 15 min) treated samples there was a decrease of around 5 times of the Cc values when compared to the CT sample. DBD treated samples obtained the lowest Cc values (~1.3×10^{-10} F/cm^2).

Table 1
Coating capacitance (Cc), E_{corr} and i_{corr} values.

Conditions	E_{corr} (V)	i_{corr} (A/cm^2)	C_c (10^{-10}F/cm^2)
CT (painted)	−0.35	1.5×10^{-7}	7.02
CT (unpainted)	−0.67	5.0×10^{-7}	–
Plasma jet			
20 s	−0.34	3.3×10^{-7}	6.71
30 s	−0.20	6.6×10^{-8}	2.45
40 s	−0.21	3.2×10^{-8}	1.80
60 s	−0.30	1.6×10^{-8}	3.00
DBD			
5 min	−0.18	3.4×10^{-8}	1.41
7.5 min	−0.11	2.4×10^{-8}	1.38
10 min	−0.13	2.7×10^{-8}	1.55
15 min	−0.11	1.9×10^{-8}	1.31

According to some authors [30,31] the coating capacitance reflects the electrolyte permeation in the coating. The smaller the diameter of the first semi-circle in the Nyquist diagram, the higher will be the solution permeation in the coating, which means that it will have higher values of Cc. On the other hand, when the first semi-circle diameter is larger, the solution permeation on the coating will be diminished and the Cc value will be smaller. Plasma treated samples obtained smaller Cc values, thus it can be inferred that the polyurethane coating on treated samples had lower electrolyte permeation when compared to the CT sample.

After EIS measurements, polarization curves experiments were conducted, the corrosion potential (E_{corr}) and current density (i_{corr}) were obtained and are shown in Table 1. One more condition was tested, the unpainted CT sample, to verify the corrosion resistance between painted and unpainted CT samples. Fig. 7 presents the polarization curves for CT, DBD and plasma jet samples.

It is possible to see that, the polyurethane paint layer on the CT substrate provided a decrease of the i_{corr} (around 3 times) and an increase of the E_{corr} from −0.67 up to −0.35 V when compared to the unpainted CT. It means that, the paint coating on the substrate has a higher corrosion resistance.

All treated samples showed i_{corr} in the order of 10^{-8} A/cm^2, except for plasma jet treated sample at 20 s. These values are about 10 to 30 times smaller than the ones of the painted and unpainted CT samples (10^{-7} A/cm^2). These results clearly indicate that the plasma exposure prior the polyurethane painting application provided even better corrosion protection onto the AA7075 alloy substrate. This fact can be attributed to the enhancement of adhesion between the polyurethane painting and the plasma treated substrate, which reduced the solution permeation in the coating. These results are in agreement with those obtained in the EIS and the adhesion tape test analyses.

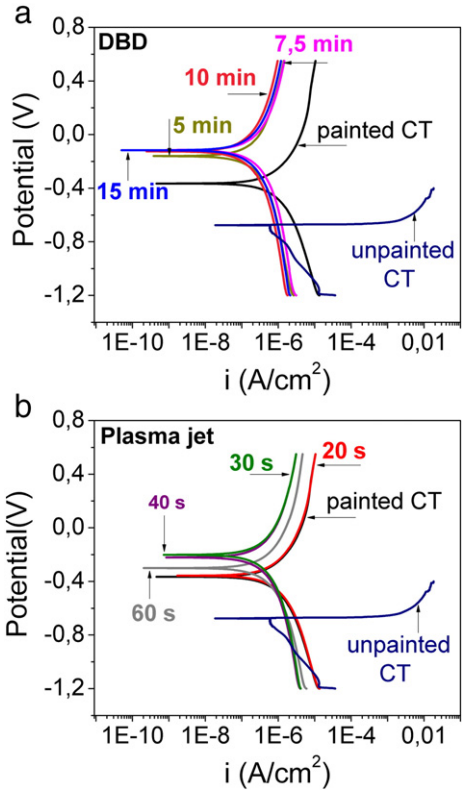

Fig. 7. Polarization curves (a) DBD (b) plasma jet.

DBD treated samples at 15 min and plasma jet at 60 s obtained the lowest values of i_{corr} (~1.6×10^{-8} A/cm^2). Corrosion potentials for DBD treated samples presented the most positives values (−0.18 up to −0.11 V) when compared to the plasma jet treated samples (−0.34 up to −0.20 V) and the painted and unpainted CT ones (−0.35 and −0.67 V).

Electrochemical corrosion analysis on uncoated plasma treated samples for each plasma process (DBD and plasma jet) was also performed. However, there was no significant variation on E_{corr}, and on i_{corr} only the plasma jet treated sample showed a slightly smaller current density. Based on the obtained results, it can be concluded that there was no significant corrosion resistance improvement on uncoated samples after plasma exposure. Therefore, plasma treatments improved only the adhesion between the PU coating and the Al alloy, and thus led to a better corrosion resistance on coated samples.

When compared to the conventional method of Al alloys anodization [32], it shows that anodized samples have a higher corrosion resistance than plasma treated ones. However, the results obtained from plasma treatment of AA7075 alloy are still positives, since plasma processing is environmental friendly and does not generate hazardous by-products. Although, it did not increase the corrosion resistance of the bare Al alloy, it enhanced significantly the adhesion of the PU coating on to the AA7075 alloy surface. Also, comparing to chromium-free coatings based on rare-earth metals [33] and sol-gel coating [34] atmospheric pressure plasma exposure of AA7075 alloy showed comparable results on adhesion enhancement.

4. Conclusions

Aluminium alloy AA7075 was treated by two types of atmospheric pressure plasma (DBD and plasma jet) to enhance the adhesion of polyurethane paint on the Al alloy surface.

The plasma treatments provided a decrease of water contact angle, an increase of surface free energy and wettability of the Al alloy samples. The excellent adhesion between the paint coating and the Al alloy surface was achieved due to the surface cleaning and activation, and not because of mechanical anchorage. From electrochemical results, it was possible to detect a lower electrolyte permeation and a higher corrosion resistance of the polyurethane painting on the AA7075 surface.

Both atmospheric pressure plasmas were efficient in improving the adhesion of the polyurethane coating on the aluminium alloy AA7075. Therefore, DBD and plasma jets are prospective and environmental friendly methods when compared to the conventional chromate processes for aluminium alloys.

Acknowledgements

This research was supported by “Coordenação de Aperfeiçoamento de Pessoal do Ensino Superior” (CAPES).

References

[1] T. Dursun, C. Soutis, Recent developments in advanced aircraft aluminium alloys, Mater. Des. 56 (2014) 862–871.
[2] E.A. Starke, J.T. Staleyt, Application of modern aluminum alloys to aircraft, Prog. Aerosp. Sci. 32 (1996) 131–172 Pergamon. Britain.
[3] Y.J. Du, M. Damron, G. Tang, H. Zheng, C.J. Chu, J.H. Osborne, Inorganic/organic hybrid coatings for aircraft aluminum alloy substrates, Prog. Org. Coat. 41 (2001) 1–6.
[4] J.-T. Qi, T. Hashimoto, J.R. Walton, X. Zhou, P. Skeldon, G.E. Thompson, Trivalent chromium conversion coating formation on aluminium, Surf. Coat. Technol. 280 (2015) 317–329.
[5] H. Shi, E.H. Han, F. Liu, S. Kallip, Protection of 2024-T3 aluminium alloy by corrosion resistant phytic acid conversion coating, Appl. Surf. Sci. 280 (2013) 325–331.
[6] K. Brunelli, L. Pezzato, E. Napolitani, S. Gross, M. Magrini, M. Dabalà, Effects of atmospheric pressure plasma jet treatment on aluminium alloys, Surf. Eng. 30 (2014).
[7] L. Bárdos, H. Baránková, Cold atmospheric plasma: sources, processes, and applications, Thin Solid Films 518 (2010) 6705–6713.
[8] O.V. Penkov, M. Khadem, W.S. Lim, D.E. Kim, A review of recent applications of atmospheric pressure plasma jets for materials processing, J. Coat. Technol. Res. 12 (2015) 225–235.
[9] H.-E. Wagner, R. Brandenburg, K.V. Kozlov, A. Sonnenfeld, P. Michel, J.F. Behnke, The barrier discharge: basic properties and applications to surface treatment, Vacuum 71 (2003) 417–436.
[10] U. Konelschatz, B. Eliasson, W. Egli, Dielectric-barrier discharges. Principle and applications, J. Phys. (1997) IV France 07. C4-47-C4-66.
[11] L. Bárdos, H. Baránková, Cold atmospheric plasma: sources, processes, and applications, Thin Solid Films 518 (2010) 6705–6713.
[12] T. Shao, C. Zhang, K. Long, D. Zhang, J. Wang, P. Yan, Y. Zhou, Surface modification of polyimide films using unipolar nanosecond-pulse DBD in atmospheric air, Appl. Surf. Sci. 256 (2010) 3888–3894.
[13] K.G. Kostov, T.M.C. Nishime, L.R.O. Hein, A. Toth, Study of polypropylene surface modification by air dielectric barrier discharge operated at two different frequencies, Surf. Coat. Technol. 234 (2013) 60–66.
[14] J.M. Jung, Y. Yang, D.H. Lee, G. Fridman, A. Fridman, Y.I. Cho, Effect of dielectric barrier discharge treatment of blood plasma to improve rheological properties of blood, Plasma Chem. Plasma Process. 32 (2012) 165–176.
[15] S. Kitazaki, T. Sarinont, K. Koga, N. Hayashi, M. Shiratani, Plasma induced long-term growth enhancement of *Raphanus sativus* L. using combinatorial atmospheric air dielectric barrier discharge plasmas, Curr. Appl. Phys. 14 (2014) S149–S153.
[16] J. Winter, R. Brandenburg, K.-D. Weltmann, Atmospheric pressure plasma jets: an overview of devices and new directions, Plasma Sources Sci. Technol. 24 (2015) 064001.
[17] M. Ghasemi, P. Olszewski, J.W. Bradley, J.L. Walsh, Interaction of multiple plasma plumes in an atmospheric pressure plasma jet array, J. Phys. D. Appl. Phys. 46 (2013) 052001.
[18] A. Van Deynse, P. Cools, C. Leys, R. Morent, N. De Geyter, Surface modification of polyethylene in an argon atmospheric pressure plasma jet, Surf. Coat. Technol. 276 (2015) 384–390.
[19] G.Y. Park, S.J. Park, M.Y. Choi, I.G. Koo, J.H. Byun, J.W. Hong, J.Y. Sim, G.J. Collins, J.K. Lee, Atmospheric-pressure plasma sources for biomedical applications, Plasma Sources Sci. Technol. 21 (2012) 043001.
[20] A.L. Santos, E.C. Botelho, K.G. Kostov, P.A.P. Nascente, L.L.G. Da Silva, Atmospheric plasma treatment of carbon fibers for enhancement of their adhesion properties, IEEE Trans. Plasma Sci. 41 (2013) 319–324.
[21] T.S.M. Mui, L.L.G. Silva, V. Prysiazhnyi, K.G. Kostov, Polyurethane paint adhesion improvement on aluminium alloy treated by plasma jet and dielectric barrier discharge, J. Adhes. Sci. Technol. 30 (2016) 218–229.
[22] ASTM D3359-07, Standard Test Methods for Measuring Adhesion by Tape Test, 2013 1–7.
[23] V. Prysiazhnyi, V. Zaporojchenkob, H. Kerstenc, M. Černák, Influence of humidity on atmospheric pressure air plasma treatment of aluminium surfaces, Appl. Surf. Sci. 258 (2012) 5467–5471.
[24] L. Bónová, A. Zahoranová, D. Kováčik, M. Zahoran, M. Mičušík, M. Černák, Atmospheric pressure plasma treatment of flat aluminum surface, Appl. Surf. Sci. 331 (2015) 79–86.
[25] J.D. Guthrie, B.J. Sparr, Infrared reflectance spectra of oxide films on aluminum-magnesium alloys, Thin Solid Films 43 (1977) 303–309.
[26] B. Díaz-Benito, F. Velasco, Atmospheric plasma torch treatment of aluminium : improving wettability with silanes, Appl. Surf. Sci. 287 (2013) 263–269.
[27] V. Prysiazhnyi, P. Vasina, N.R. Panyala, J. Havel, M. Cernak, Air DCSBD plasma treatment of Al surface at atmospheric pressure, Surf. Coat. Technol. 206 (2012) 3011–3016.
[28] G.W. Walter, The application of impedance spectroscopy to study the uptake of sodium chloride solution in painted metals, Corros. Sci. 32 (1991) 1041–1058.
[29] A.S.L. Castela, A.M. Simões, M.G.S. Ferreira, E.I.S. evaluation of attached and free polymer films, Prog. Org. Coat. 38 (2000) 1–7.
[30] J. Wang, Y. Zuo, Y. Tang, The study on Mg-Al rich epoxy primer for protection of aluminum alloy, Int. J. Electrochem. Sci. 8 (2013) 10190–10203.
[31] F. Fredrizzi, F.J. Rodriguez, S. Rossi, F. Deflorian, R.D. Maggio, The use of electrochemical techniques to study the corrosion behaviour of organic coatings on steel pretreated with sol-gel zirconia films, Electrochim. Acta 46 (2001) 3715–3724.
[32] A. Hakimizad, K. Raeissi, F. Ashrafizadeh, A comparative study of corrosion performance of sealed anodized layers of conventionally colored and interference-colored aluminium, Surf. Coat. Technol. 206 (2012) 4628–4633.
[33] P.S. Coloma, U. Izagirre, Y. Belaustegi, J.B. Jorcin, F.J. Cano, N. Lapeña, Chromium-free conversion coatings based on inorganic salts (Zr/Ti/Mn/Mo) for aluminum alloys used in aircraft applications, Appl. Surf. Sci. 345 (2015) 24–35.
[34] S. Beraa, T.K. Routb, G. Udayabhanua, R. Narayanc, Comparative study of corrosion protection of sol-gel coatings with different organic functionality on Al-2024 substrate, Prog. Org. Coat. 88 (2015) 293–303.